

Stabilized zirconia-based planar sensor using coupled oxide(+Au) electrodes for highly selective CO detection

Anggraini, Sri A.

Interdisciplinary Graduate School of Engineering Sciences, Kyushu University

Plashnitsa, Vladimir V.

Research and Education Center of Carbon Resources, Kyushu University | Department of Chemistry and Biochemistry, University of Notre Dame

Elumalai, Perumal

Department of Materials Science, School of Chemistry, Madurai Kamaraj University

Breedon, Michael

Japan Society for the Promotion of Science

他

<https://hdl.handle.net/2324/25682>

出版情報 : Sensors and Actuators B : Chemical. 160 (1), pp.1273-1281, 2011-12-15. Elsevier B.V.
バージョン :
権利関係 : (C) 2011 Elsevier B.V.



Stabilized Zirconia-based Planar Sensor Using a Couple of Oxide(+Au) Electrodes for Highly Selective CO Detection

Sri A. Anggraini,^a Vladimir V. Plashnitsa,^{b,1} Perumal Elumalai,^e

Michael Breedon,^{d,e} and Norio Miura^{e,*}

*^aInterdisciplinary Graduate School of Engineering Sciences, Kyushu University,
Kasuga-shi, Fukuoka 816-8580, Japan*

*^bResearch and Education Center of Carbon Resources, Kyushu University,
Kasuga-shi, Fukuoka, 816-8580, Japan*

*^cDepartment of Materials Science, School of Chemistry, Madurai Kamaraj University,
Madurai, Tamilnadu, 625021, India*

^dJapan Society for the Promotion of Science, Tokyo 102-8421

*^eArt, Science and Technology Center for Cooperative Research, Kyushu University,
Kasuga-shi, Fukuoka, 816-8580, Japan*

*Corresponding author. Tel: +81-92-583-8852; Fax: +81-92-583-8976

E-mail address: miurano@astec.kyushu-u.ac.jp (N. Miura)

Present addresses:

¹Department of Chemistry and Biochemistry, University of Notre Dame, Notre Dame,
Indiana, 46545, USA (V.V. Plashnitsa).

Abstract

A mixed-potential-type yttria-stabilized zirconia (YSZ)-based planar sensor utilizing coupled oxide(+Au) electrodes was developed with aspirations of highly selective and sensitive carbon monoxide (CO) detection. The combination of a $\text{Nb}_2\text{O}_5(+\text{Au})$ -sensing electrode (SE) and a $\text{NiO}(+\text{Au})$ -SE' in one sensor at an operational temperature of 450°C was found to be capable of cancelling out high responses to NO_x and unsaturated hydrocarbons (HCs), while maintaining a response to CO. The present combined-type sensor demonstrated a linear relation of the CO sensitivity with the logarithm of CO concentration in the range of 10–400 ppm, providing a rather high response, even down to 10 ppm CO. The polarization curves obtained for the combined-type sensor indicated that the sensing mechanism involved a mixed potential at both of the composite electrodes; $\text{Nb}_2\text{O}_5(+\text{Au})$ -SE and $\text{NiO}(+\text{Au})$ -SE'. In addition, the CO sensitivity of the combined-type sensor was invariant to changes in water vapor concentration in the range of 2–11 vol.%.

Keywords: CO sensor, Mixed potential, YSZ, Nb_2O_5 , NiO, gold

1. Introduction

An efficient combustion process will be marked by a complete conversion of hydrocarbons (HCs) to CO_2 and H_2O , while an incomplete conversion leads to a formation of undesirable gas species, such as carbon monoxide (CO). Due to its high toxicity, and with an ever increasing awareness in the importance of controlling air pollution from different combustion processes, the development of reliable and high-performance CO sensor is of the utmost importance. With challenges in maintaining stability under harsh environments, solid-electrolyte-based electrochemical gas sensors have been proven as suitable candidates for exhaust sensing applications [1-4]. Yttria-stabilized zirconia (YSZ)-based gas sensors are considered to be one of the leading candidates for reliable and robust devices and having been studied extensively over the past decade for exhaust gas detection [1-5].

Many efforts have been undertaken to implement different sensing electrode (SE) materials as well as optimizing the sensing performance of solid-state electrochemical sensors, aiming at obtaining high sensitivity and selectivity to CO [6-31]. However, most of these sensors were unable to generate a CO response without interference from coexisting gases, such as saturated and unsaturated HCs, and/or NO_x . [6-8,14,16,21,28,29]. This is due to the similar behavior of YSZ-based sensors toward these gases, arising mixed-potential at SE. For HCs in particular, the response magnitude increases with the increasing number of carbon atoms per molecule [31-32]. This, therefore, often results in larger electromotive force

(*emf*) response to hydrocarbons (especially with high carbon atoms number) rather than CO, giving unsatisfactory CO selectivity. Nevertheless, it has been recently reported that a YSZ-based sensor using Nb₂O₅-SE could be considered as a potential candidate for the CO detection [26], while giving the cross-sensitivity to HCs [21].

So far, there have been few reports on YSZ-based sensors capable of achieving good CO selectivity [20, 22, 24]. Among them, a planar-like YSZ-based sensor, which had been reported by our group, using the combination of CdO and SnO₂ sensing electrodes demonstrated an ability to detect CO rather sensitively and selectively at high temperature [24]. This YSZ-based sensor utilized a single CdO-SE (*emf* was measured vs. Pt/air-reference electrode (RE)) was able to provide a relatively high sensitivity, but somewhat unselective response to CO. To cancel out high cross-sensitivity to other interfering gases, CdO-SE was coupled with SnO₂-SE', which has a rather small CO response (vs. Pt/air-RE) [24]. This technique appears to be a promising strategy in obtaining a highly-selective CO sensor. However, CdO is well-known as a hazardous material, and the substitution of CdO-SE with any non-poisonous material should be preferentially considered in the construction of a reliable, environmentally-friendly, sensitive and selective CO sensor.

In this present study, the sensing performance of a YSZ-based sensor utilizing a Nb₂O₅-SE for CO detection was initially optimized via the addition of different amounts of Au (5-15 wt.%) into the sensing layer. As an additive, Au was chosen here because of its proven favorable influence on the enhancement of gas-sensing properties in YSZ-based

sensors [6-14,26,28-31]. It was found that addition of 10 wt.% Au into Nb₂O₅-SE significantly improved both the sensitivity towards CO and the sensitivities to all other gases examined. To suppress high responses to NO_x and HCs (especially, propene), Nb₂O₅(+Au)-SE was coupled with NiO(+Au)-SE', which has been reported by our group as a suitable material for sensitive and selective detection of C₃H₆ at high temperature [32]. As a result, the fabricated combined-type YSZ-based planar sensor using a pair of composite Nb₂O₅(+Au)-SE and NiO(+Au)-SE' was found to be able to detect CO rather sensitively and selectively at 450°C under humid conditions. The CO sensing characteristics and the proposed sensing mechanism of the obtained combined-type sensor are further reported in this paper.

2. Experimental

2.1 Fabrication of single- and combined-type planar sensors

A tape-casted YSZ plate (8 mol.% Y₂O₃-doped zirconia) with the physical dimensions of 10 mm squared and 0.2 mm in thickness was used for the fabrication of both single- and combined-type sensors. The schematic view of the single-type YSZ-based sensor is shown in Fig. 1 (a). Here, each different commercial oxide powder (Nb₂O₅, Ta₂O₅, SnO₂ and Co₃O₄; Wako Pure Chemical Industries Ltd., Japan) was thoroughly mixed with α -terpineol and then

screen-printed on the front side of the YSZ plate to form an oxide-SE with average thickness of about 4 μm . The obtained oxide-printed YSZ plate was dried at 130°C overnight and sintered at 1000°C for 2 h in air. In addition, the composite Nb_2O_5 (+ 5-15 wt.% Au)-SEs were also obtained by mixing Nb_2O_5 with the appropriate amount of Au powder (0.3-0.6 μm , Nilaco Corp., Japan) under sonication in ethanol for 3 h.

The fabrication process and thermal treatment for each of the composite Nb_2O_5 (+Au)-SEs were the same as mentioned above. The Pt layer formed on the back side of YSZ plate was used as the RE. Thus, the single-type planar sensors, fabricated and evaluated in the present study, can be expressed as:

(+) Oxide-SE / YSZ / Pt-RE (–) , (Sensor A)

(+) Nb_2O_5 (+Au)-SE / YSZ / Pt-RE (–) . (Sensor B)

The use of dissimilar electrodes has been reported elsewhere [32, 33, 34, 35].

As it is indicated, each of the SEs was connected to the positive terminal of digital electrometer (R8240, Advantest Corp., Japan) with a high input impedance ($>10\text{ G}\Omega$); conversely the Pt-RE was connected to the negative terminal.

As for the combined-type sensor (Fig. 1 (b)), the composite Nb_2O_5 (+10 wt.% Au)- and NiO (+6 wt.% Au)-SEs were applied parallel with each other on the same side of YSZ plate. Here, there was no Pt-RE and the present combined-type sensor was assigned as:

(+) Nb_2O_5 (+Au)-SE / YSZ / NiO (+Au)-SE' (–), (Sensor C)

where Nb_2O_5 (+Au)-SE was connected to the positive terminal of the digital electrometer and NiO (+Au)-SE' was connected to the negative terminal.

2.2 Evaluation of sensing characteristics.

The gas-sensing characteristics of the fabricated planar sensors (both single and combined types) were evaluated in a conventional gas-flow apparatus equipped with an electric furnace operating at 450-500°C. Each of the sensors was exposed to either a humid base gas (5 vol.% O₂ + 5 vol.% water vapor + N₂ balance), or the sample gas that was prepared by diluting each of parent gases (CO, CH₄, C₃H₈, C₃H₆, NO and NO₂) with the base gas. The total gas flow-rate was fixed at 100 cm³·min⁻¹ during all measurements. During the gas selectivity tests, the concentration of each of the examined gases in the sample gas was kept constant at 400 ppm. The responses to various CO concentrations were examined in the range of 10 – 400 ppm. The *emf* output between oxide-SE and Pt-RE (Sensors A and B) or between Nb₂O₅(+ 10 wt.% Au)-SE and NiO(+ 6 wt.% Au)-SE' (Sensor C) was measured as a sensing signal. The gas sensitivity (Δemf) was defined as the difference between the *emf* value of sensor in the sample gas (*emf_{sample}*) and that in the base gas (*emf_{base}*).

The measurement of current-voltage (polarization) curves for each of the single- and combined-type sensors was performed using an electrochemical analyzer (PGSTAT30, AutoLab[®], Echo-Chemie, The Netherlands). The polarization curves were measured in potentiodynamic mode, with a constant scan rate of 3 mV·min⁻¹. The surface morphology of SE materials was observed via a field-emission scanning-electron microscope (FE-SEM,

JEOL, JSM-340F).

3. Results and Discussion

3.1 Morphologies of electrode surfaces

Morphological SEM observations of both sensing electrodes materials after calcination at 1000°C for 2 h were performed. The SEM surface images of Nb₂O₅ and NiO, are shown in Fig. 2 (a) and (b), respectively. The Nb₂O₅ material presented in Fig. 2 (a) was found to have a slightly porous surface, when compared with NiO. Particles were laminar in shape, with grain diameters ranging from 200 nm to 2 – 5 µm. Whereas, the morphology of NiO was observed to be comparatively denser, comprised of spherical particles with an average grain size ranging from 165 nm up to 2 µm. The gold distribution over the oxide material is depicted in Fig. 2 (c) and (d) as back-scattering (BS) SEM images for Nb₂O₅(+10 wt.% Au)-SE and NiO(+6 wt.% Au)-SE, respectively; where bright spots are representative of higher atomic weight element; gold particles. The gold particles were found to be evenly dispersed over both metal oxide electrodes. After calcining at high temperature, some of the gold particles that were originally 300-600 nm in diameter coalesced into larger particles of a few µm in diameter. It is seen that the particle size of Au on Nb₂O₅ is relatively higher than that on NiO.

3.2 Sensing characteristics of the single-type sensors

Prior to selection of the most suitable SE material to be used for development of highly selective and sensitive CO sensor, several metal oxides were tested as SE in the single-type planar sensor (Sensor A). Figure 3 shows the comparison of cross sensitivities to various gases at 500°C under humid conditions (5 vol.% water vapor) for the single-type sensors utilizing different oxide-SEs. It can be seen that the sensor using SnO₂-SE or Nb₂O₅-SE gave a rather high response to 400 ppm CO. The CO response of the sensor attached with SnO₂-SE was, however, found to be unstable under the present operating condition, in comparison with Nb₂O₅-SE. While the level of CO sensitivity, and most importantly the selectivity for the sensor attached with Nb₂O₅-SE should be improved, Nb₂O₅ could still be considered as a prospective candidate of SE material for further study of CO sensing.

The enhancement of the CO sensing characteristics for the Nb₂O₅-SE based sensor was attempted by the addition of Au powder (5, 10 and 15 wt.%) into the Nb₂O₅ used for electrode fabrication. Figure 4 show the cross sensitivities to various gases at 450°C under humid conditions for the single-type sensors (Sensor B) using the Au-added Nb₂O₅-SEs. The sensing characteristics for the sensor using the parent Nb₂O₅-SE is also shown in Fig. 4 for comparison. Here, particular attention has been focused on an attaining high CO sensitivity as

well as good temporal stability of the Au-added Nb₂O₅-SEs examined, regardless of their lack of selectivity. It is seen from Fig. 4 that the addition of Au into the Nb₂O₅-SE has improved the sensitivity to CO. The addition of 5 wt.% and 10 wt.% Au into Nb₂O₅-SE resulted in an almost tripled CO sensitivity. However, the addition of 15 wt.% of gold into Nb₂O₅-SE decreased the CO sensitivity. The difference between the CO sensitivity for these composite SEs was insignificant (around ± 10 mV). Despite these similar gas-sensing characteristics, the sensor attached with Nb₂O₅(+10 wt.% Au)-SE [denoted, Nb₂O₅(+Au)-SE] was experimentally confirmed to provide a more stable CO response at 450°C under humid conditions, when compared with Nb₂O₅(+5 wt.% Au)-SE. Thus, the CO sensing characteristics of the sensor using Nb₂O₅(+Au)-SE was further examined.

The results in Fig. 4 can be attributed to the Au distribution observed in Fig. 5 (a-c). The addition of Au particles, as observed on the surface of Nb₂O₅(+5 wt.% Au) in Fig. 5 (a), has increased the response to CO significantly. Figure 5 (b) is representative of the Nb₂O₅(+10 wt.% Au)-SE surface which was observed to have both small (300-600 nm), and larger coalesced Au particles (approximately 2 μ m); this had a CO response similar in magnitude with the sensor using Nb₂O₅(+ 5 wt.% Au). However, at 15 wt.% additions of Au, a significantly greater number of smaller particles coalesced into larger particles (Fig. 5 (c)), correlating with a lower CO response.

Figure 6 (a) shows the *emf*-response transients to various CO concentrations in the range of 10 – 400 ppm for the sensor using Nb₂O₅(+Au)-SE operated at 450°C under humid

conditions. Once the sensor was exposed to the sample gas containing CO, the *emf* signal was swiftly changed from the base line and reached the steady-state *emf* value in due time. Then, upon the introduction of the base gas over the sensor, the *emf* value returned quickly to the original base level. It should be emphasized that the sensor using Nb₂O₅(+Au)-SE was able to offer high sensitivity even to 10 ppm CO at 450°C. Each Δemf point in Fig.6 was calculated by subtracting the maximum *emf* value recorded for each individual CO concentration, and the baseline *emf* value prior to the introduction of CO gas to the gas testing cell. The CO sensitivity (Δemf) of the sensor varied logarithmically with the CO concentration, as shown in Fig. 6 (b). Such behavior is usually observed for mixed-potential-type sensors, as reported elsewhere [1,24,32].

The establishment of mixed potential can be rationalized by the measurements of polarization (current–voltage) curves. By using a modified polarization curve, the mixed potential that arises at the SE/YSZ interface can be confirmed mathematically. The mixed potential is defined as the potential where the cathodic and anodic curves intersect on a modified polarization curve [33]. The polarization curve measurements for the sensors using Nb₂O₅-based-SEs were conducted in the base gas (5 vol.% O₂ + N₂ balance) and in the sample gas (400 ppm CO + 5 vol.% O₂ + N₂ balance) at 450°C in humid conditions. The measurements were performed with respect to Pt-RE by applying a linearly increasing sweep potential over a defined range, and measuring the generated current.

Here, the reactions (1) and (2) proceed simultaneously at SE/YSZ interface, causing

the development of a mixed-potential. The obtained polarization curves for the cathodic reaction of oxygen



and the modified polarization curves for the anodic reaction of CO



are shown in Fig. 7.

The polarization curves displayed in Fig. 7 (a) and Fig. 7 (b) are the original unmodified polarization curves of the sensors using Nb₂O₅-SE and Nb₂O₅(+Au)-SE respectively. For clarity, the O₂ polarization curve has been divided into two regions in both Fig. 7 (a) and Fig. 7 (b). The O₂ polarization curve bracketed by the A1-O₂ and the B1-O₂ regions represent the range where O₂ reduction occurs. While, the O₂ polarization curves in the A2-O₂ and the B2-O₂ regions correspond to regions of positive current, where O₂ evolution occurs.

The CO+O₂ polarization curve is divided into three regions in both figures; A1-(CO+O₂), A2-(CO+O₂) and A3-(CO+O₂) regions in Fig. 7 (a); as well as B1-(CO+O₂), B2-(CO+O₂), and B3-(CO+O₂) in Fig. 7 (b). The A1-(CO+O₂) and the B1-(CO+O₂) represent regions where O₂ reduction and CO oxidation occur. The negative current value indicates that the O₂ reduction reaction is more dominant than the CO oxidation reaction. The decreasing current value (with respect to the same point on the O₂ polarization curve) indicates that CO oxidation indeed occurs, given that the oxidation reaction would generate a

positive current flow in the opposite direction of O_2 reduction reaction, thus the measured total (net) current of both reactions would be decrease when compared with the O_2 reduction reaction alone. The A2-(CO+ O_2) and B2-(CO+ O_2) regions also correspond to the O_2 reduction and the CO oxidation reactions. Here, the CO oxidation reaction appears to proceed at a relatively higher rate than the O_2 reduction reaction, as indicated by the positive direction of the measured current. The A3-(CO+ O_2) and the B3-(CO+ O_2) represent the CO oxidation reaction and the O_2 evolution reaction which is expected to occur in this region. However, any changes of measured current do not correspond with changes in O_2 catalytic activity of the electrode. Since the measurements were carried out under identical testing conditions (except for the introduction of CO gas during the CO+ O_2 measurement), the O_2 catalytic activity is believed to be unchanged. Therefore, the increasing current represents the CO oxidation current.

In order to obtain the modified polarization curve, the CO+ O_2 curve was subtracted from the cathodic curve of O_2 . The resulting modified polarization curves (Fig. 7 (c)) were attained by plotting the potential value for CO and the potential value for O_2 with the absolute current value ($|I|$). The intersection point of these polarization curves for the sensor using pure Nb_2O_5 -SE is indicated as $E_{Nb_2O_5}$ and that for the sensor attached with $Nb_2O_5(+Au)$ -SE is displayed as $E_{Nb_2O_5(+Au)}$. As seen from this Fig. 7(c), the addition of 10 wt.% Au into Nb_2O_5 -SE drastically increased the catalytic activity to the anodic reaction involving CO (2). At the same time, the Au addition also brought about a slight decrease in the catalytic activity

to the cathodic reaction of O_2 (1). These changes in catalytic activities resulted in the shift of intersection point in a negative direction ($E_{Nb_2O_5} \rightarrow E_{Nb_2O_5(+Au)}$), giving a larger mixed-potential value for the sensor using the composite $Nb_2O_5(+Au)$ -SE. Since both electrochemical reactions (1) and (2) proceed at the SE/YSZ interface, it appears that the role of Au at the interface is to promote the catalytic activity to the CO anodic reaction (2) and to suppress the catalytic activity of the O_2 cathodic reaction (1); indicated by the increase in CO sensitivity after Au addition. These effects are likely to occur as a result from not only the modified electrochemical catalytic activity of the Nb_2O_5 -SE, but also the decrease in catalytic activity toward CO oxidation over the sensing electrode (gas-phase reaction). If the catalytic activity towards the gas-phase reaction decreases, then the concentration of CO gas reaching the interface of SE/YSZ will increase, resulting in a larger mixed potential.

However, when the Au concentration was raised above 10 wt.%, gold particles are suspected to coalesce during the calcination process and forming larger sized Au particles, as depicted in Fig. 5 (b) and (c) where larger Au particles were observed in relatively greater number on the surface of $Nb_2O_5(+15 \text{ wt.} \% \text{ Au})$ -SE than $Nb_2O_5(+10 \text{ wt.} \% \text{ Au})$ -SE. As the Au particle size increases, the surface area and the number of available reaction sites will decrease until the particles have a similar catalytic properties to that of bulk gold, which seems to be relatively inert under the operating conditions examined in this study. Thus, the size/surface area relationship is considered to be responsible for the declining CO sensitivity observed with the addition of 15 wt.% of Au into Nb_2O_5 -SE.

It should be noted that both mixed potentials ($E_{\text{Nb}_2\text{O}_5}$ (-160 mV) and $E_{\text{Nb}_2\text{O}_5(+\text{Au})}$ (-310 mV)) estimated from the polarization-curve measurements were found to be close to those (-152 mV and -327 mV, respectively) obtained experimentally. These estimated results from the polarization curves correlate well with the empirical results indicating that the present sensors are working based on the mixed-potential mechanism. At the mixed potential point, both CO oxidation and O₂ reduction reactions arise and proceed at an equal rate (steady state) which is indicated by the zero current at the mixed-potential point. This is consistent with the result of our polarization curve measurement where the current value at mixed potential is zero. In Fig. 7 (a) for example, at the mixed potential (around -160 mV) the current for O₂ is -30 nA, whereas the current for CO+O₂ is zero. This zero current value does not indicate that current is zero or that current is not flowing, because current is actually flowing between the reduction and oxidation reactions at equal rate in opposing direction (\pm 30 nA).

Although the addition of Au has proven to be effective in enhancing the CO sensitivity of the sensor attached with Nb₂O₅-SE, the CO selectivity was, however, unimproved. Higher response to CO also brought about higher responses to other coexisting gases, especially saturated (C₃H₈) and unsaturated (C₃H₆) HCs as well as NO₂. Based on the above-mentioned results, the achievement of high CO selectivity for the single-type sensor (where the potential of SE is measured against Pt-RE) seems to be difficult and it should be accomplished via alternative means.

3.3 Sensing characteristics of the combined-type sensor

Recently, our group has reported about highly sensitive, selective and stable C₃H₆ sensor using a composite NiO(+Au)-SE operated at 600°C [32]. Thus, the combination of NiO(+Au) electrode together with Nb₂O₅(+Au)-SE in one planar sensor is expected to minimize the responses to coexisting gases, while keeping the level of CO sensitivity sufficiently high.

In the present study, by controlling the Au addition (3-15 wt.%) into NiO-SE, the single-type sensor using NiO (+6 wt.% Au)-SE [hereinafter, NiO(+Au)-SE'] was found to exhibit relatively low response to CO and nearly match the same level of C₃H₆ sensitivity that was observed for the sensor using Nb₂O₅(+Au)-SE at 450°C. Based on this finding, a combined-type planar sensor (Sensor C, Fig. 1 (b)) consisting of a coupled Nb₂O₅(+Au)-SE and NiO(+Au)-SE' was fabricated and its sensing characteristics were evaluated at 450°C under humid conditions. Figure 8 shows the comparison of cross sensitivities to different gases at 450°C under humid conditions for the single-type sensors attached with each of (a) Nb₂O₅(+Au)-SE and (b) NiO(+Au)-SE', and (c) for the combined-type sensor using coupled Nb₂O₅(+Au)-SE and NiO(+Au)-SE'. It can be seen that both single-type sensor electrodes (Nb₂O₅(+Au)-, NiO(+Au)-SE) vs. Pt-RE gave non-selective response, however high responses to C₃H₆ and NO₂ were observed. The similarity of these responses together with the

significant difference in CO response leads to high CO selectivity and sensitivity for the combined-type sensor ($\text{Nb}_2\text{O}_5(+\text{Au})\text{-SE}$ vs. $\text{NiO}(+\text{Au})\text{-SE}'$, Fig. 8 (c)).

Figure 9 (a) shows the *emf*-response transient to different CO concentrations in the range of 10 – 400 ppm for the combined-type sensor using coupled $\text{Nb}_2\text{O}_5(+\text{Au})\text{-SE}$ and $\text{NiO}(+\text{Au})\text{-SE}'$ operated at 450°C under humid conditions. The present sensor gave stable and repeatable response to each CO concentration. It should be also noted that the sensitivity to 10 ppm CO was as high as -50 mV. Figure 9 (b) exhibits the dependence of the sensitivity (Δemf) on the logarithm of gas concentration for the combined-type sensor. It is seen that Δemf observed for NO and C_3H_6 varied non-linearly with the logarithm of gas concentration, indicating the complexity of chemical and electrochemical processes at both oxide (+Au) electrodes. Whereas, the CO sensitivity varied almost linearly with the logarithm of gas concentration in the range of 10 – 400 ppm, confirming the occurrence of a mixed-potential at both $\text{Nb}_2\text{O}_5(+\text{Au})\text{-SE}$ and $\text{NiO}(+\text{Au})\text{-SE}'$.

Verification of the established mixed-potential for the combined-type sensor was confirmed by the measurements of polarization (*I-V*) curves both in the base gas and in the sample gas containing 400 ppm CO at 450°C. The original cathodic and the modified anodic polarization curves obtained for the cathodic reaction (1) and anodic reaction (2), respectively, are depicted in Fig. 10. For comparison, the polarization curves for the single-type sensor attached with each of $\text{Nb}_2\text{O}_5(+\text{Au})\text{-SE}$ and $\text{NiO}(+\text{Au})\text{-SE}'$ (vs. Pt-RE) are also shown in Fig. 10. Each cathodic polarization curve intersects with each modified anodic polarization

curve at a certain potential, corresponding to E_1^m for the potential of $\text{Nb}_2\text{O}_5(+\text{Au})\text{-SE}$ vs. Pt-RE , E_2^m for $\text{NiO}(+\text{Au})\text{-SE'}$ vs. Pt-RE and E_3^m for $\text{Nb}_2\text{O}_5(+\text{Au})\text{-SE}$ vs. $\text{NiO}(+\text{Au})\text{-SE'}$. It is clearly seen that the difference (-137 mV) between E_1^m and E_2^m is in good agreement with the difference (-130 mV) between E_3^m value and the potential value measured in the base gas (referred as E_3^{base} in Fig. 10). Such a close agreement confirms the suitability of the mixed-potential mechanism for the single-type and combined-type sensors.

To prove the capability of the combined type sensor in terms of a practical application, the influence of water vapor on the CO sensitivity was examined. The measurements were performed in the range of 2–11 vol.% water vapor, covering all possible variations of water vapor concentration in a real automobile exhaust. Figure 11 shows the dependence of sensitivity to 400 ppm CO on the change in water vapor concentration for the present combined-type sensor operated at 450°C. It can be seen that Δemf is nearly constant in the examined water vapor concentration range. The relatively invariant response to changes in water vapor concentration is one of the highly desirable performance characteristic from the viewpoint of the potential practical application of this sensor.

4. Conclusions

Attractive CO gas-sensing characteristics (high sensitivity and selectivity to CO, insensitivity to change in water vapor concentration) have been achieved by means of the

combination of composite $\text{Nb}_2\text{O}_5(+\text{Au})$ and $\text{NiO}(+\text{Au})$ electrodes in one YSZ-based planar sensor operated at 450°C under humid conditions (5 vol.% water vapor). The addition of Au in appropriate amount to $\text{Nb}_2\text{O}_5\text{-SE}$ has been proven to increase the catalytic activity to anodic reaction of CO which results in improving CO sensitivity. The proposed combined-type YSZ-based sensor was able to provide selective, sensitive and repeatable response to each CO concentration examined, exhibiting relatively high sensitivity (ca. 50 mV) even to 10 ppm CO. The sensitivity (Δemf) varied linearly with the logarithm of CO concentration in the range of 10–400 ppm, indicating the establishment of mixed-potential, which was also confirmed by the polarization-curve measurements. Our efforts are currently focused on solving the remaining practical aspects, i.e. reproducibility and long-term stability. It is well-known that these two parameters are of a critical importance for YSZ-based sensors using pure Au-SEs [16, 29]. Thus, there should be further screening of single-phase oxide SEs as possible substitutive analogues of Au-doped composite SEs, as described above.

Acknowledgements

This work was supported by the Kyushu University Global-COE Program on “Novel Carbon Resource Sciences”, Grant-in-Aid for Scientific Research (B) (22350095) and for JSPS Fellows (22-00353).

References

- [1] N. Miura, P. Elumalai, V. Plashnitsa, T. Ueda, R. Wama, and M. Utiyama, *Solid State Gas Sensing*, p.182, Springer, New York (2009)
- [2] C. O. Park, Solid-state electrochemical gas sensors, J. W. Fergus, N. Miura, J. Park, A. Choi, *Ionics*, **15**, 261 (2009)
- [3] R. Moos, A brief overview on automotive exhaust gas sensors based on electroceramics, *Intern. J. App. Ceramic Tech.*, **2**, 401 (2005)
- [4] P. Pasierb, M. Rekas, Solid-state potentiometric gas sensors-current status and future trends, *J. Solid State Electrochem*, **13**, 3 (2009)
- [5] J. W. Fergus, Sensing mechanism of non-equilibrium solid-electrolyte-based chemical sensors, *Sens. Actuators B:Chem.*, **122**, 683 (2007).
- [6] R. Wu, C. Hu, C. Yeh, P. Su, Nanogold on powdered cobalt oxide for carbon monoxide sensor, *Sens. Actuators B:Chem.*, **96**, 596 (2006).
- [7] J. Zosel, D. Tuchtenhagen, K. Ahlborn, U. Guth, Mixed-potential gas sensor with short response time, *Sens. Actuators B:Chem.*, **130**, 326 (2008).
- [8] R. Mukundan, E. L. Brosha, D. R. Brown, F. H. Garzon, A mixed-potential sensor based on a $\text{Ce}_{0.8}\text{Gd}_{0.2}\text{O}_{1.9}$ electrolyte and platinum and gold electrodes, *J. Electrochem. Soc.*, **147**, 1583 (2000).
- [9] S. Thiemann, R. Hartung, U. Guth, U. Schönaauer, Chemical modifications of

- Au-electrodes on YSZ and their influence on the non-nernstian behaviour, *Ionics*, **2**, 463 (1996).
- [10] J. Zosel, D. Westphal, S. Jakobs, R. Muller, U. Guth, Au-oxide composites as HC-sensitive electrode material for mixed potential gas sensors, *Solid State Ionics*, **152-153**, 525 (2002).
- [11] J. Zosel, R. Muller D. Westphal, V. Vashook, U. Guth, Response behavior of perovskites and Au/oxide composites as HC-electrodes in different combustibles, *Solid State Ionics*, **175**, 531 (2004).
- [12] D. Westphal, S. Jakobs and U. Guth, Gold-composite electrodes for hydrocarbon sensors based on YSZ solid electrolyte, *Ionics*, **7**, 182 (2001).
- [13] P. Shuk, E. Bailey, J. Zosel, U. Guth, New advanced in site carbon monoxide sensor for the process application, *Ionics*, **15**, 131 (2009).
- [14] A. Morata, J. P. Viricelle, A. Tarancon, G. Dezanneau, C. Pijolat, F. Peiro, J. R. Morante, Development and characterization of a screen-printed mixed potential gas sensor, *Sens. Actuators B: Chem.*, **130**, 561 (2008).
- [15] N. Wu, M. Zhao, J. Zheng, C. Jiang, B. Myers, S. Li, M. Chyu, S. X. Mao, Porous CuO-ZnO nanocomposite for sensing electrode of high-temperature CO solid-state electrochemical sensor, *Nanotechnology*, **16**, 2878 (2005).
- [16] R. Mukundan, E. L. Brosna, D. R. Brown, F. H. Garzon, Ceria-electrolyte-based mixed potential sensors for the detection of hydrocarbons and carbon monoxide,

- Electromchem. Solid-state Lett.*, **2**, 412 (1999).
- [17] X. Li, K. T. Jacobs and G. M. Kale, La-doped Ba₂In₂O₅ electrolyte: Pechini synthesis, microstructure, electrical conductivity, and application for CO gas sensing, *J. Electrochem. Soc.*, **157**, J285 (2010).
- [18] K. Mochizuki, R. Sorita, H. Takashima, K. Nakamura, G. Lu, Sensing characteristics of a zirconia-based CO sensor made by thick-film lamination, *Sens. Actuators B:Chem.*, **77**, 190 (2001).
- [19] N. Li, T. C. Tan, H. C. Zeng, High-temperature carbon monoxide potentiometric sensor, *J. Electrochem.Soc.*, **140**, 1068 (1993).
- [20] R. Sorita, T. Kawano, A highly selective CO sensor using LaMnO₃ electrode-attached zirconia galvanic cell, *Sens. Actuators B:Chem.*, **40**, 29 (1997).
- [21] L. Chevallier, E. Di Bartolomeo, M.L. Grilli, E. Traversa, High temperature detection of CO/HCs gases by non-nernstian planar sensors using Nb₂O₅ electrode, *Sens. Actuators B:Chem.*, **130**, 514 (2008).
- [22] X. Li, G. M. Kale, Influence of thickness of ITO sensing electrode film on sensing performance of planar mixed potential CO sensor, *Sens. Actuators B:Chem.*, **120**, 150 (2006).
- [23] X. Li, G. M. Kale, Influence of sensing electrode and electrolyte on performance of potentiometric mixed-potential gas sensors, *Sens. Actuators B:Chem.*, **123**, 254 (2007).
- [24] N. Miura, T. Raisen, G. Lu, N. Yamazoe, Highly selective CO sensor using stabilized

- zirconia and a couple of oxide electrodes, *Sens. Actuators B:chem.*, **47**, 84 (1998).
- [25] J. Park, A. Azad, S. Song, E. D. Wachsman, Titania-based miniature potentiometric carbon monoxide gas sensors with high sensitivity, *J. Am. Ceram. Soc.*, **93**, 742 (2010).
- [26] L. Chevallier, E. DiBartolomeo, M. L. Grili, M. Mainas, B. White, E.D. Wachsman, E. Traversa, Non-nernstian planar sensors based on YSZ with a Nb₂O₅ electrode, *Sens. Actuators B:Chem.*, **129**, 591 (2008).
- [27] F. H. Garzon, R. Mukundan, E. L. Brosha, Solid-state mixed potential gas sensors: theory, experiments and challenges, *Solid State Ionics*, **136-137**, 633 (2000)
- [28] J. Zosel, K. Ahlborn, R. Müller, D. Westphal, V. Vashook, U. Guth, Selectivity of HC-sensitive electrode materials for mixed potential gas sensors, *Solid State Ionics*, **169**, 115 (2004).
- [29] T. Hibino, A. Hashimoto, S. Kakimoto, M. Sano, Zirconia-based potentiometric sensors using metal oxide electrodes for detection of hydrocarbons, *J. Electrochem.Soc.*, **148**, H1 (2001)
- [30] T. Hibino, Y. Kuwahara, S. Wang, S. Kakimoto, M. Sano, Nonideal electromotive force of zirconia sensors for unsaturated hydrocarbon gases, *Electrochem. Solid-state Lett.*, **1**, 197 (1998).
- [31] T. Hibino, S. Kakimoto, M. Sano, *J. Electrochem. Soc.*, **146**, 3361 (1999).
- [32] P. Elumalai, V.V. Plashnitsa, Y. Fujio, N. Miura, Highly sensitive and selective stabilized zirconia-based mixed-potential-type propene sensor using NiO/Au composite

- sensing-electrode, *Sens. Actuators B:Chem.*, **144**, 215 (2010).
- [33] N. Miura, Y. Yan, G. Lu, N. Yamazoe, Sensing characteristics and mechanism of hydrogen sulfide sensor using stabilized zirconia and oxide sensing electrode, *Sens. Actuators B:Chem.*, **34**, 371 (1996).
- [34] N. Miura, K. Kurosawa, M. Hasei, G. Lu, N. Yamazoe, Stabilized zirconia-based sensor using oxide electrode for detection of NO_x in high-temperature combustion exhaust, *Solid State Ionics*, **86**, 88, (1996).
- [35] T. Hibino, S. Wang, S. Kakimoto, M. Sano, Detection of propylene under oxidizing conditions using zirconia-based potentiometric sensor, *Sens. Actuators B: Chem.*, **50**, 149 (1998).

Biographies

Sri Ayu Anggraini received her MSc degree in environmental science from Graduate School of Frontier Science, the University of Tokyo in 2007. She is currently a doctor course student in Kyushu University. Her research interests are focused on the development of high-performance gas-sensing devices based on stabilized zirconia and oxide sensing-electrodes.

Vladimir V. Plashnitsa received his MSc degree in Electrochemical Engineering from the Vyatka State Technical University, Russia in 1997 and PhD degree in Materials Science (Dr. rer. nat.) from the Max-Planck-Institute for Metal Research, Stuttgart, Germany in 2004. In 2004 – 2010, he was employed as Postdoctoral Research Associate and then as Research Assistant Professor in Kyushu University, Fukuoka, Japan. Currently, he is working as Postdoctoral Research Associate in the Laboratory of Low Dimensional Nanomaterials, Department of Chemistry and Biochemistry, University of Notre Dame, Notre Dame, USA. His research interests are focused on solid state chemistry and electrochemistry, nanomaterials and nanocomposites, and different multi-functional ceramic materials for various devices (solar cells, sensors for exhaust and environmental controls batteries, etc.).

Perumal Elumalai received his MSc degree in Chemistry from Muthurangam Govt. Arts College, Vellore, India in 1997 and PhD degree from the Solid State & Structural Chemistry Unit, Indian Institute of Science, Bangalore, India in 2004. During 2004-2009, he worked as a post-doctoral fellow in Arts, Science and Technology Center for Cooperative Research, Kyushu University, Japan. Currently, he is Assistant Professor in School of Chemistry, Department of Materials Science, Madurai Kamaraj University, Madurai, India. His research interests are on high temperature gas sensors, alkaline and Li-ion batteries, supercapacitors, electrocatalysis, nanomaterials and solid-state electrochemistry.

Michael Breedon received his two Bachelor of Applied Science (Chemistry and Nanotechnology) degrees and PhD from RMIT University, Melbourne, Australia. He is currently undertaking a JSPS Postdoctoral Fellowship at Kyushu University, Japan investigating high temperature YSZ based gas sensors, novel aqueous synthesis methods, and computational modeling. His research interests include gas sensors, aqueous chemical synthesis, density functional theory simulations of gas adsorption, electron microscopy, nanotechnology, materials science, and advanced material applications.

Norio Miura has been a professor at Kyushu University, Japan since 1999. He received BE degree in Applied Chemistry in 1973, ME degree in 1975 from Hiroshima University, Japan and PhD degree in Engineering in 1980 from Kyushu University. His current research

concentrates on development of high-performance gas sensors (e.g. solid-state electrochemical sensors for automotive exhaust and environmental gases) as well as new functional materials (e.g., electrodes of electrochemical super capacitors and oxide-based selective oxygen sorbents).

Figure captions

Fig. 1 Schematic representations of (a) the single-type YSZ-based planar sensor using an oxide-SE and Pt-RE, and (b) the combined-type sensor comprised of a coupled $\text{Nb}_2\text{O}_5(+\text{Au})$ -SE and $\text{NiO}(+\text{Au})$ -SE'.

Fig. 2 Representative SEM images of electrode surface of (a) $\text{Nb}_2\text{O}_5(+10 \text{ wt.}\% \text{ Au})$, (b) $\text{NiO}(+6 \text{ wt.}\% \text{ Au})$; and the corresponding back-scattering SEM images of (c) $\text{Nb}_2\text{O}_5(+10 \text{ wt.}\% \text{ Au})$ and (d) $\text{NiO}(+6 \text{ wt.}\% \text{ Au})$.

Fig. 3 Cross sensitivities to various gases (400 ppm each) for the single-type YSZ-based sensors utilizing different oxide-SEs at an operational temperature of 500°C under humid conditions.

Fig. 4 Cross sensitivities to various gases at 450°C under humid conditions for the single-type sensor using either pure a Nb_2O_5 -SE or Au-added Nb_2O_5 -SEs.

Fig. 5 Representative back-scattering SEM images of the electrode surface of Nb_2O_5 (a) $+5 \text{ wt.}\% \text{ Au}$, (b) $+10 \text{ wt.}\% \text{ Au}$, and (c) $+15 \text{ wt.}\% \text{ Au}$, after calcination at 1000°C for 2 h.

Fig. 6 (a) Response transients to CO and (b) dependence of the sensitivity (Δemf) on the logarithm of CO concentration in the range of 10 – 400 ppm, for a single-type sensor utilizing $\text{Nb}_2\text{O}_5(+\text{Au})$ -SE operating at 450°C .

Fig. 7 The unmodified polarization curves for (a) the sensor using Nb_2O_5 -SE and (b) the sensor using $\text{Nb}_2\text{O}_5(+\text{Au})$ -SE, and (c) the modified polarization curves for the

single-type sensors using each of Nb₂O₅-based-SEs, obtained in 5 vol.% O₂ and in 400 ppm CO at 450°C in the presence of 5 vol.% H₂O.

Fig. 8 Comparison of cross sensitivities to various gases at 450°C under humid conditions for the single-type sensors utilizing a (a) Nb₂O₅(+Au)-SE, (b) NiO(+Au)SE, or (c) the combined-type sensor using coupled Nb₂O₅(+Au)-SE and NiO(+Au)-SE'.

Fig. 9 (a) Response transient to CO and (b) dependence of the sensitivity on the gas concentration, for the combined-type sensor attached with coupled Nb₂O₅(+Au)-SE and NiO(+Au)-SE' operated at 450°C under humid conditions.

Fig. 10 Polarization curves obtained both in 5 vol.% O₂ and in 400 ppm CO for the single-type sensors using each of Nb₂O₅(+Au)-SE and NiO(+Au)-SE and for the combined-types sensor using coupled Nb₂O₅(+Au)-SE and NiO(+Au)-SE'.

Fig. 11 Dependence of the sensitivity (Δ emf) to 400 ppm CO on water vapor concentration in the range of 2-11 vol.% for the combined-type sensor using coupled Nb₂O₅(+Au)-SE and NiO(+Au)-SE' at an operational temperature of 450°C.

Figure 1

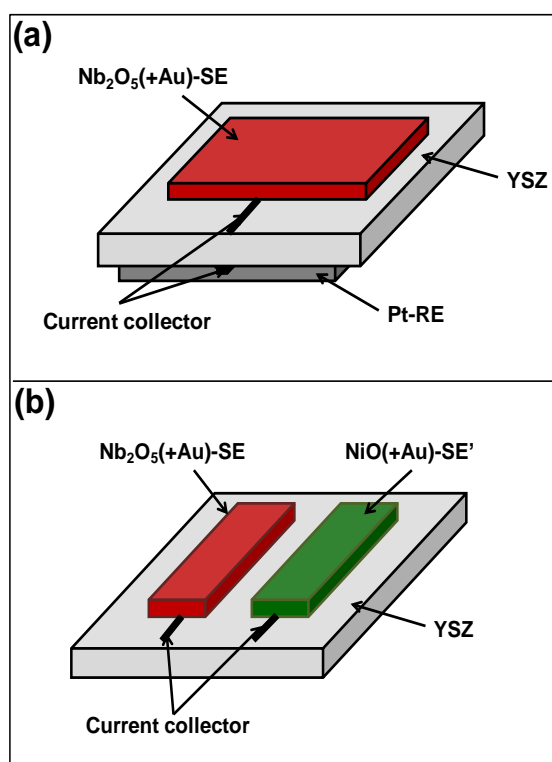


Figure 2

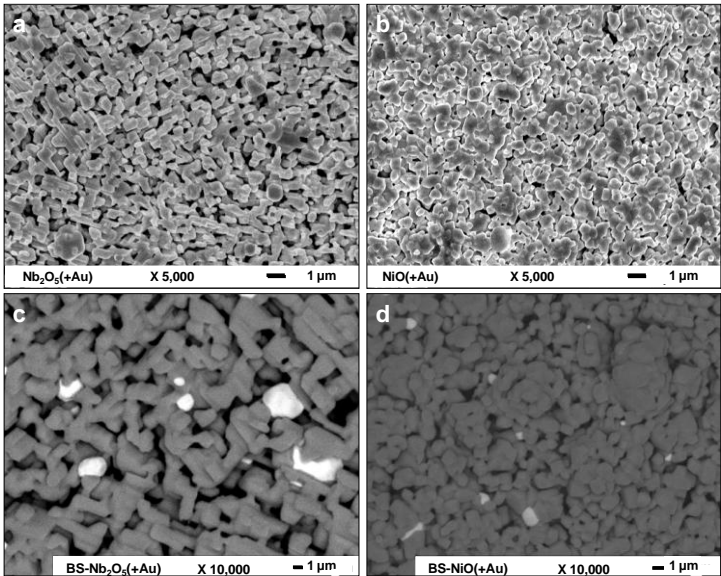


Figure 3

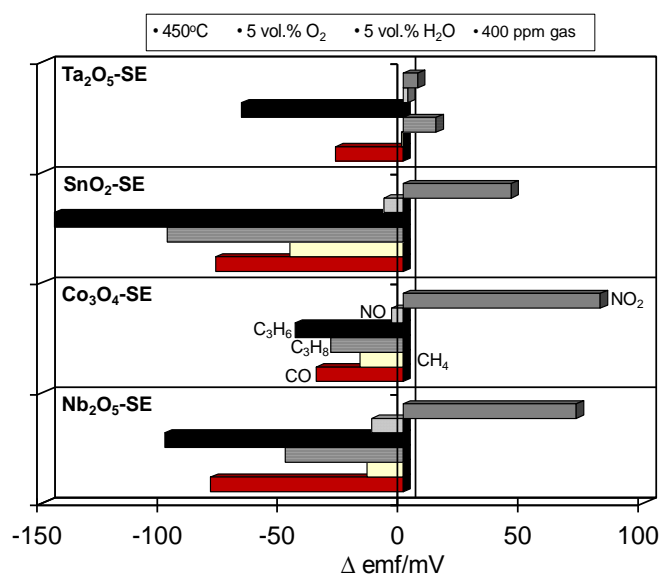


Figure 4

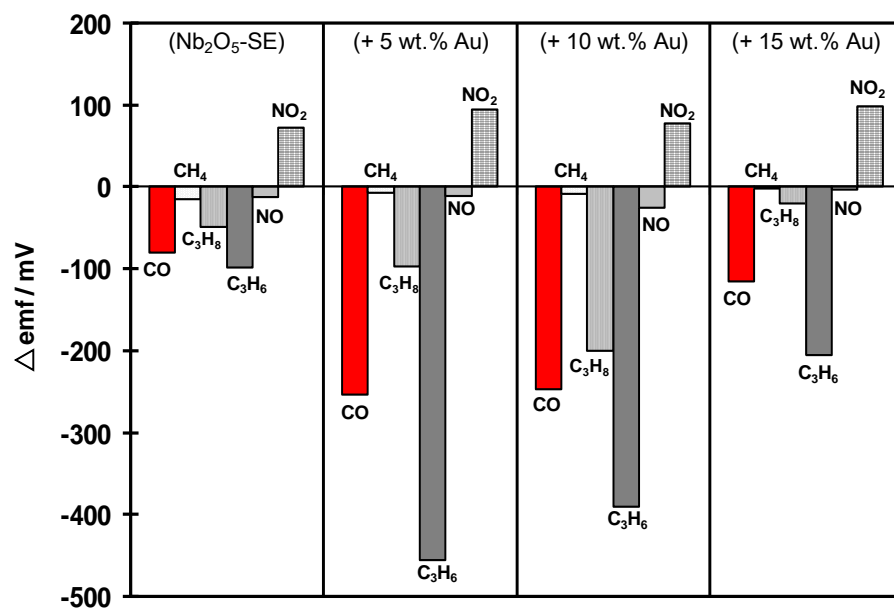


Figure 5

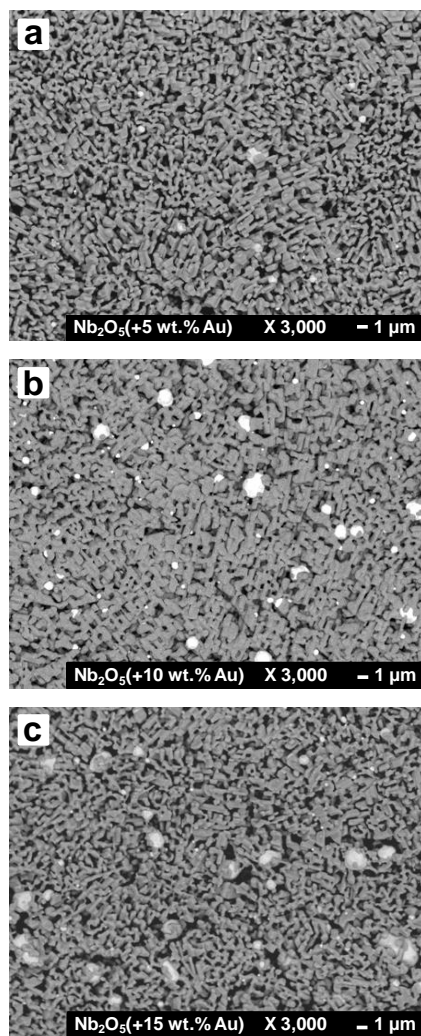


Figure 6

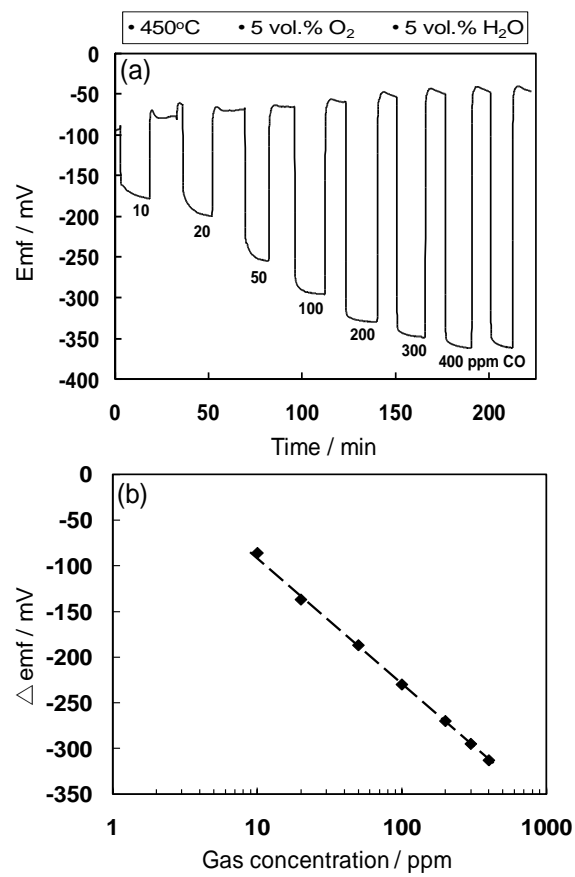


Figure 7

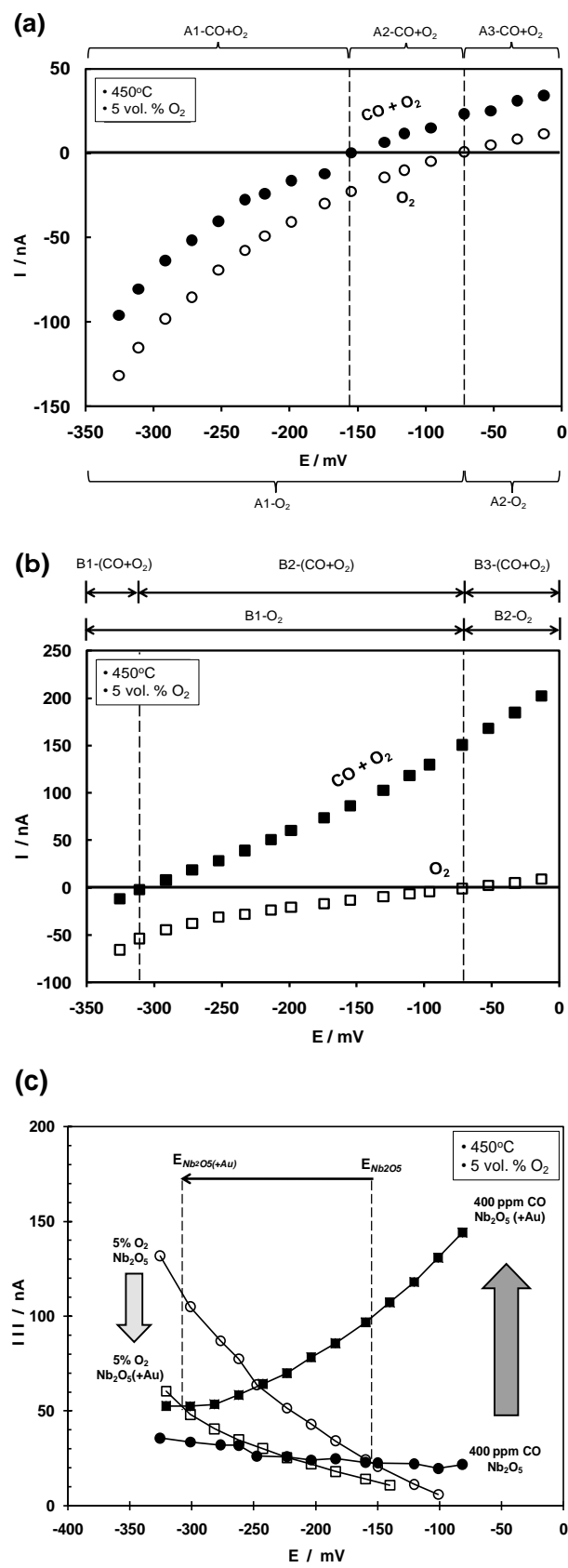


Figure 8

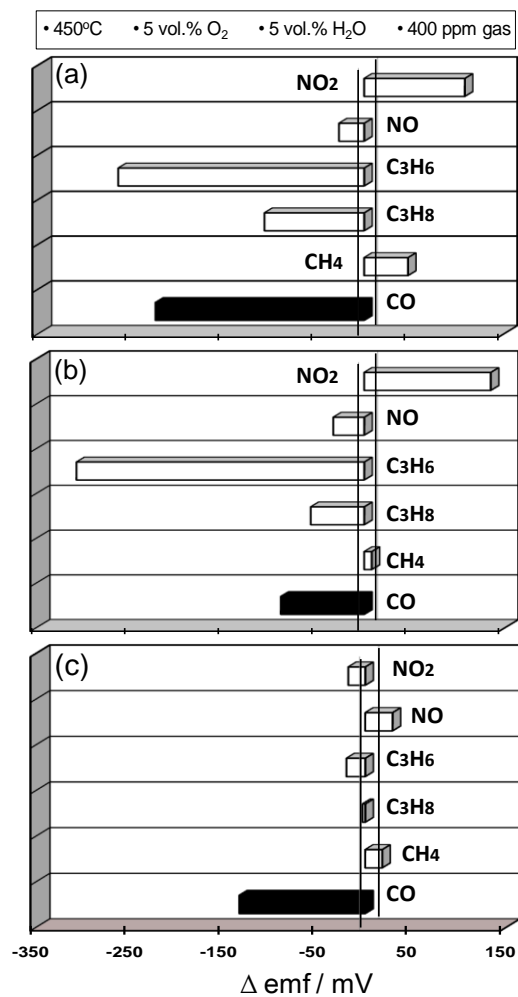


Figure 9

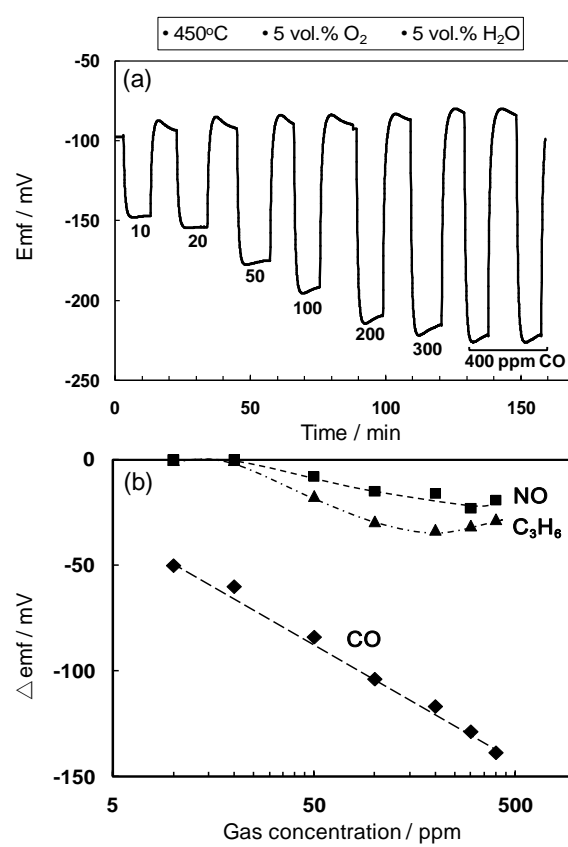


Figure 10

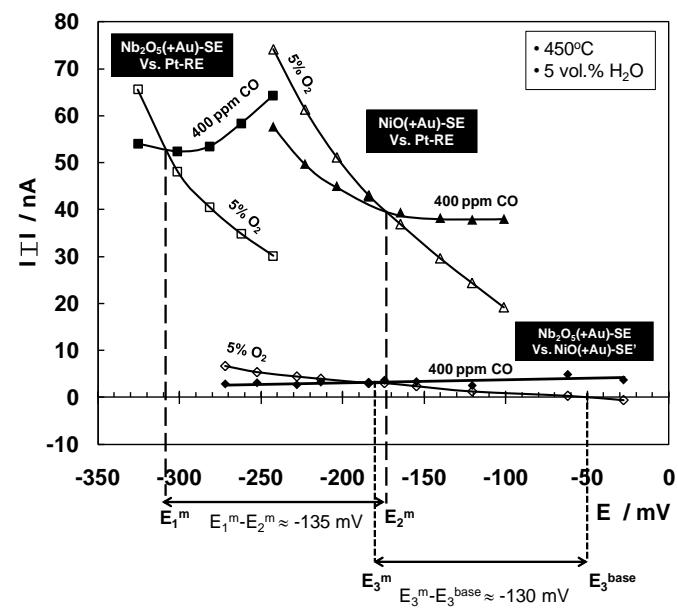


Figure. 11

